International Symposium of Research Students on Materials Science and Engineering
December 20-22, 2004, Chennai, India
Department of Metallurgical and Materials Engineering Indian Institute of Technology Madras

KINETICS OF CARBON DISSOLUTION IN FERROSILICON ALLOYS

Pedro J. Yunes
School of Material Sciences and Engineering, University of New South Wales, Sydney, Australia

ABSTRACT

Carbon dissolution plays an important role for interpreting the interaction between silicon and carbon during the melting process. Reported data about solubility of carbon in semiconductor and solar-grade silicon had been published for several authors. There are also some findings during the ferrosilicon manufacturing process, establishing changes in carbon content in several grades of ferrosilicon 75. However, kinetic data of the carbon dissolution in ferrosilicon alloys were not available. In the present work, carbon solubility in ferrosilicon alloys containing 25,75 and 98.5% Si in equilibrium with synthetic graphite at 1550 °C are shown. In addition, wettability studies using the sessile droplet method were carried out for the above mentioned ferrosilicon alloys on graphite. In order to have a better understanding of the interfacial phenomena during the interaction metal droplet – substrate, microscopy research was also undertaken showing the formation of SiC phase after a short reaction period.

Keywords: ferrosilicon – kinetics –graphite – wettability

1. INTRODUCTION

Ferrosilicon lumps and coke are two important components of the charge on any metal scrap-based process. In the cupola process, the major exothermic reactions involve the carbon contained in coke and the oxygen in the blast. There is also some carbon going into the liquid metal. Carbon content has a major influence on almost all physical and mechanical properties and it is the most influential element in any cast iron. Silicon plays equally an important role as graphitizer and ferritizer in cast iron and it is usually added as ferrosilicon.

Since the metallic charge melts and metal droplets are mixed up with coke lumps in the reaction chamber, the study of reaction kinetics and surface parameters bring a better understanding of the overall process. It is known when silicon content increases, solubility of carbon in liquid iron decreases. However, information available is mainly for low silicon content in the metal.
The solubility of carbon in silicon had been addressed for several authors, and was found to be very low [1-6]. Most of those results were obtained at different temperatures and using semiconductor and solar-grade silicon, which contain very low presence of impurities. From thermodynamical data were also established very low carbon contents in equilibrium with silicon for different ferrosilicon alloys [7,8].

Wetting data of silicon and ferrosilicon alloys on silicon carbide under different conditions had been published in the literature [9-12]. Values oscillated from 0 to 45° at temperatures ranging from 1683 to 1770 °K. However, little if any information was found about kinetics of carbon dissolution on ferrosilicon alloys under metallurgical conditions. The same applies for wetting studies, where most of the findings were focused in bonding properties of different metals on

SiC, but not certainly, for the interfacial phenomena of ferrosilicon alloys on carbonaceous materials.
In the present work is presented the carbon saturation limits found in Si (98.5%), FeSi75 and FeSi25. An attempt to find the mechanism of carbon dissolution for silicon alloys with higher silicon contents is explained. In addition, wettability studies using drop-sessile method were undertaken and dynamic wetting for the above-mentioned alloys on synthetic graphite is shown, as well interfacial studies between ferrosilicon – graphite.

2. PREVIOUS STUDIES

Scace et al [2] carried out some experiments to find the solubility of C in liquid Si at temperatures up to 2900° C as well as a proposed phase diagram for the system. Nozaki et al [3] conducted some experiments using semiconductor silicon at the silicon melting point and found the carbon concentration just prior to the appearance of silicon carbide was $3.5 \pm 0.4 \times 10^{17}$ at./ cm^3. Yanaba et al [6] found a temperature dependence of the carbon solubility in liquid silicon [1].

$$\text{Log (C/mass\%)} = 3.63 - 9660/T \quad (\pm 0.02) \quad (T: 1723 - 1873\ K) \quad [1]$$

and therefore, carbon solubility at the melting point of silicon was calculated to be 79 ppm (9.1×10^{18} at/ cm^3). Summary of experimental conditions and results obtained from early work published shown [6] some differences, probably because the effect of some dissolved oxygen in the metal. The oxygen impurities in the melt disturb the Si/SiC equilibrium due to the formation of SiO_2 at the Si/SiC interface.

Ottem [7] obtained thermodynamic data for the solubility of carbon in pure silicon, FeSi75 and FeSi65. It seems at 1550 °C, solubility of Si is around 150 – 170 ppm, while values for FeSi75 (100 – 120 ppm) and FeSi65 (70 – 75 ppm) are lower and showed a correlation between Silicon content and dissolved Carbon in the metal.

Study undertaken by Klevan [8] found contains of 700 -1100 ppmw C when FeSi75 is tapped from the furnace. Statistical analyses of 779 shipments over 3 years found that the carbon content dropped to an average of 300 ppmw C, after vesting, crushing and screening the material. This implies that the Carbon, which precipitates as SiC particles as the temperature drops during tapping and handling, is physically removed as particles to a fairly large extent, but there is still a way to go before the solubility limit of 70 ppm C at 1500°C is reached.

Reported values of contact angle between Silicon and Silicon Carbide were compiled from different authors and shown on Table 1.

Kalogeropoulos et al. [12] measured the wettability of α-SiC by FeSi using two different compositions (33.33 and 66.67 at% Si). The contact angle measured was 35º for both alloys at their respective melting points

3. EXPERIMENTAL METHODS AND MATERIALS

3.1 Materials

Several ferrosilicon alloys, ranging from 25 to 98.5 % were used on the experiments. It was not possible to contact any manufacturer able to supply Ferrosilicon in the whole range neither with a low level of impurities. So, it was necessary to produce the ferroalloys from high purity raw materials (Iron, chips 99.98%, No. 26,794-5 and Silicon, lump, 98.5%, No. 26,742-2, Aldrich Chemical Company, Inc.)

Raw materials were weighted and calculations were made in order to obtain desired compositions (25 and 75% Si) as close as possible. They were melted using a laboratory-scale arc melter, currently used to make metallic alloys under strict compositions. Before the melting started, the entire system was checked to prevent any leakage, as well as, sucking any remaining air created a vacuum. A gas stream (10% Hydrogen, 90% Argon) was supplied in order to keep a reductant atmosphere and prevent any further oxidation.

Further chemical analyses, using a GBC Integra ICP-AES instrument with 22-channel polychromator and monochromator, were carried out to check chemical compositions. Carbon contents were obtained from the Carbon-Sulphur Analyser (LECO CS 444).

(Table 2) Synthetic graphite crucibles (ID = 10 mm, H ≈ 12 – 15 mm) were used for carbon dissolution experiments. Synthetic graphite plates (24 x 24 x 2 mm) were used as substrates for wettability experiments.

3.2. Experimental Apparatus

The experimental arrangement used for the experimental work had been widely described in the literature [13,14]. (Fig 1) A horizontal high temperature furnace, which includes a 50 mm inner diameter high alumina reaction tube, sealed with water-cooled brass caps at two ends was used. Super Kanthal resistance heating elements heat the furnace. The temperature is measured by a thermocouple inside of the reaction tube close to the sample. For contact angle experiments, the liquid sample is monitored in-situ at high temperature with a TV/VCR unit connected to a CCD camera, which permits the capture of images of the metal droplets. This arrangement makes it possible to measure the contact angle between sample and the substrate. Images obtained can be processed using software. A high purity argon stream was introduced through an inlet at one cap and off gas is released at the other cap. In order to remove any moisture and Oxygen contained in the gas, a purifier gas system was currently used [15].

Ferroalloys samples were crushed and placed into the crucibles. For wettability experiments, sample weighed around 0.1 gram. Samples were placed in the reaction tube near the cap where the temperature is near the room temperature and push into the hot zone, were temperature was 1550° C. The time the samples were held into the hot zone ranged from 30 seconds up to 6 hours.

After samples cooled down, graphite crucibles were removed from the sample using sand paper. Samples were cleaned with alcohol and air blowed and then, ready to be analysed in the carbon analyser (LECO).

For interfacial studies, metallographic samples were cross-section cut, mounted on a bakelite substrate, polished and cooper coated. Images and chemical analysis were obtained from electron probe micro analyser (EPMA) Cameca SX 50.

4. RESULTS AND DISCUSSION

4.1 Carbon solubility

Data from literature [7] established there is a direct correlation between silicon content and carbon saturation in the ferroalloy, although those results were obtained for silicon contents from 65% Si onwards. Fig 2 shows that carbon content increased within minutes for the whole range of samples tested up to reach the equilibrium values.

Carbon content increased very quickly within minutes and saturation was reached currently after 2 - 3minutes. The saturation limit was the highest for FeSi25, ranging around 0.13 – 0.14 %C. Lower saturation values were observed for other ferrosilicon alloys tested, with overall values around 0.10 %C for Si and 0.09 %C for FeSi75. From some "finger" experiments using pure iron on graphite, carbon saturation rose 5.5 wt% in close agreement with data reported from previous work [17] .It is very likely the iron plays a role increasing the carbon saturation, since the carbon solubility is considerably higher than silicon.

The kinetic mechanism proposed includes liquid-side mass transfer and chemical reaction.
A first-order equation was applied [2] , based on the assumption that dissolution of carbon was controlled by liquid-side mass transfer.

$$\frac{dC}{dt} = \frac{kA}{V}(Cs - Ci) \quad [2]$$

The integrated form of [2], introducing an overall carbon dissolution rate constant (K in s^{-1}) is shown in [3]

$$\ln\frac{(Cs - Ct)}{(Cs - Co)} = -Kt \quad [3]$$

Where Cs, Ct and Co are the melt carbon saturation, the instantaneous melt carbon content and the initial carbon content respectively. Experimental data plotted from Si runs are shown on Fig 3 and showed good agreement with equation [3].

4.2 Wettability and Interfacial studies

Results from sessile-drop experiments were are showed on Fig 4 . Dynamic wetting in Si occurred at the fastest rate (Fig 5a,5b,5c), followed by FeSi75 (Fig 6a,6b,6c) until full wetting is reached. However, after a sharp decrease in contact angle during the first 2-3 minutes, values remained quite stable around 60 ° for FeSi25. (Fig 7a,7b,7c)

Although carbon pickup might occur due to liquid mass-transfer mechanism in first place, some interfacial reaction also occurred. It is very likely the formation of SiC on the interface occur according to [4].

$$Si + C = SiC \quad [4]$$

Images from EPMA in the interface showed the formation of SiC on the interface metal-graphite (Fig 8,9,10). This process it would be also associated to the dynamic wetting observed, since it is reported good wetting between Si and SiC.

As it was discussed earlier, carbon dissolves very fast on silicon and ferrosilicon alloys. Carbon saturation is reached in very short time, after the first 1 – 3 minutes, depending of the composition. After this period, no significant changes were detected and it was assumed that equilibrium was reached. At the same time, quick changes in contact angle were observed. It seems both process takes place almost simultaneously and the formation of SiC layer is responsible for decelerating the process of carbon transferred into the metal. This fact could also explain the dynamic wetting, since SiC has high adhesion energy and good wetting, therefore, fast decreasing of contact angle occurred while its formation occurred.

5. CONCLUSIONS

1. Kinetics of carbon dissolution in silicon and ferrosilicon alloys occurs due to a liquid – side mass transfer mechanism. At early stages, carbon dissolution process occurred during the first 1 – 3 minutes, but afterwards, the process slowed down because of formation of SiC occurred in the interface.
2. Presence of iron-rich phase seems to be the responsible for increasing the carbon saturation limit when silicon content in the ferroalloy is lower.
3. Full wetting occurred for Si and FeSi75 within 1 minute. Sharp decreasing in contact angle for FeSi25 was observed but final contact angle value remained around 60 °. Results from interfacial studies showed the formation of SiC on the interface and explained the good wetting for high silicon alloys.

ACKNOWLEDGMENTS

The author would like to thanks the financial support provided from Tyco Water, Australia, as well as the valuable help from Mr. Russell Bush, Technical Manager of Tyco Water facility at New South Wales, Australia.

REFERENCES

1. R. N. Hall, *J. Appl. Phys*. 29 (1958) 914
2. R. I. Scace , G. A. Slack , *J. Chem. Phys*. 30 (1959) 1551
3. T. Nozaki,Y. Yatsurugi, N. Akiyama, *J. Electrochem. Soc*.117 (1970) 1566
4. L.L. Oden ,R.A. McCune, *Met. Trans. A*, 18A (1987) 2005
5. K. Sakaguchi , M. Maeda, *Met. Trans. B*, 23B (Aug 1992) 423
6. K. Yanaba, M. Akasaka, M. Takeuchi, M.Watanabe, T. Narushima ,Y. Iguchi, *Mat. Trans., JIM*, 38, 11 (1997) 990.
7. L. Ottem, *Løselighet og termodynamiske data for oksygen og carbon I flytende legeringer av silisium og ferrosilisium*, SINTEF report STF34 F93027 (1993) pp. 43
8. O.S. Klevan, *Removal of C and SiC from Si and FeSi during ladle refining and solidification*. Dr. Ing. Thesis, 1997.
9. J.V. Naidich, *Progress in surface and Membrane Science*, 14 (1981) 428
10. K. Nogi, K. Ogino, *Wettability of Silicon Carbide by Liquid Metals. Proc. Int. Symp. On Advanced Structural Materials*, D.S. Wilkinson. (1988)
11. P. Nikolopoulos, S.Agathopoulos, G. N. Angelopoulos, A. Naoumidis , H. Grübmeier, *J. Mat. Sci*., 27 (1992) 139.
12. S. Kalogeropoulos, L. Baud, N. Eustathopoulos, *Acta Metall. Mater*. 43(3) (1995) 907
13. F. McCarthy,*Wettability of Refractory Materials by Fe-C-S Alloys*. BSc Thesis. University of New South Wales (1997)
14. A.S.Mehta, *Wettability and Reaction Occuring at the slag/carbon Interface during Pulverised Coal Injection in a Blast Furnace*. Ph.D Thesis. University of New South Wales (2000)
15. E.Kapilashrami, *Reactions Between Oxygen – Containing Iron Melts and Dense Alumina or Silica.* PhD Thesis. Royal Institute of Technology,Stocholm (2001).
16. Wu,C; Sahajwalla, V. *Met.Trans. B*. 31B (April 2000) 243

17. Zhao,L, *Interfacial Phenomena and Chemical reactions during interactions of Iron and graphite/Oxide substrates for refractory applications*. PhD Thesis. University of New South Wales (2003)

TABLES

Table 1. Contact angle of Si(l) on SiC. Reported Values.

Reference	θ (º)	Temperature (K)
Naidich [9]	36	1753
Naidich [9]	42	1703
Nogi et al. [10]	0	1773
Nikilopoulos et al. [11]	38	1683 / 1770
Nikilopoulos et al.[11]	41.5	1740

Table 2. Chemical compositions of materials

	Fe	Si	C	Al
FeSi25	72.6-75.2	24.6-26	0.012-0.034	0.06
FeSi50	49.5-50.4	49.2-51.6	0.015-0.033	0.08
FeSi75	22.7-26.7	72.2-76.8	0.015-0.024	0.06

FIGURES

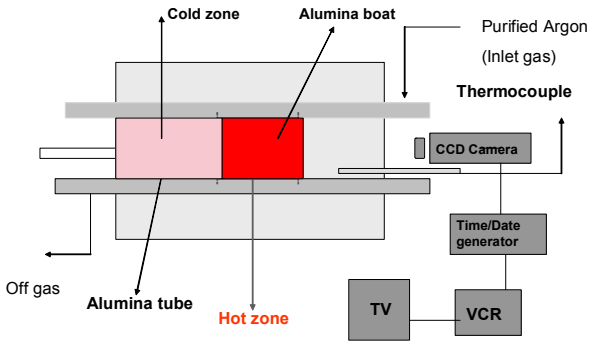

Fig 1. Schematic of the experimental arrangement

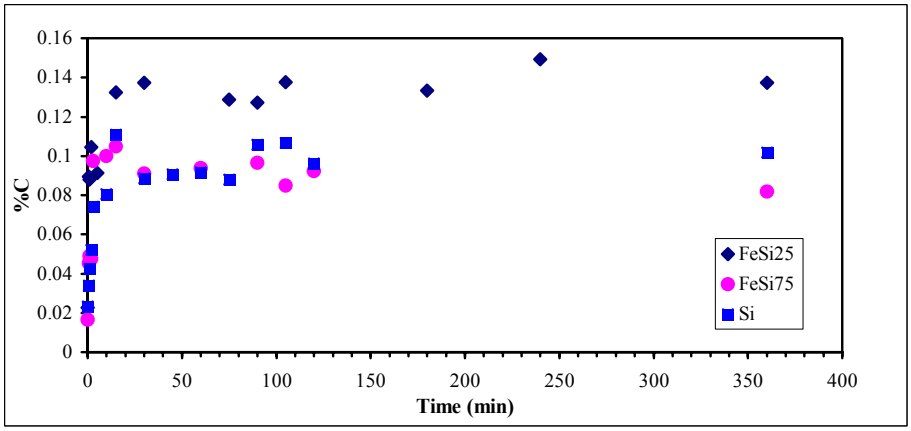

Fig 2.Change of Carbon content for different ferrosilicon alloys

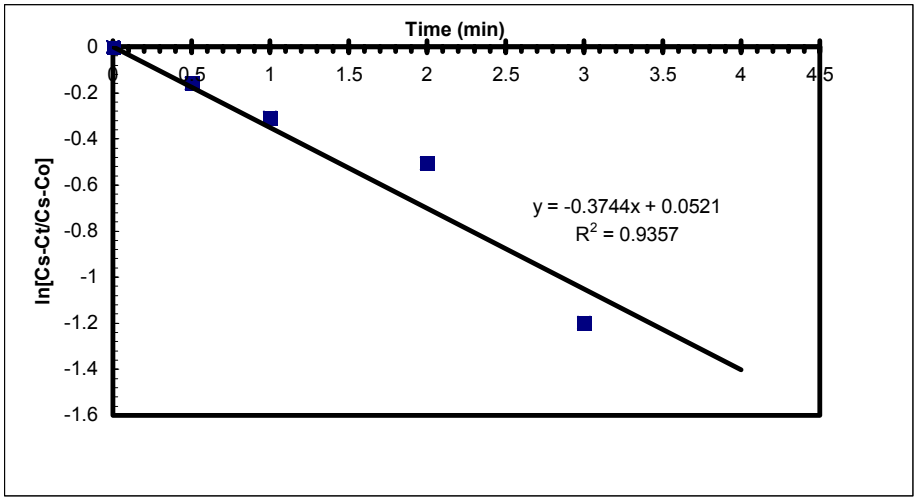

Fig 3 Plot of ln (Cs-Ct/Cs-Co) against time for dissolution of synthetic graphite in molten silicon at 1550 °C.

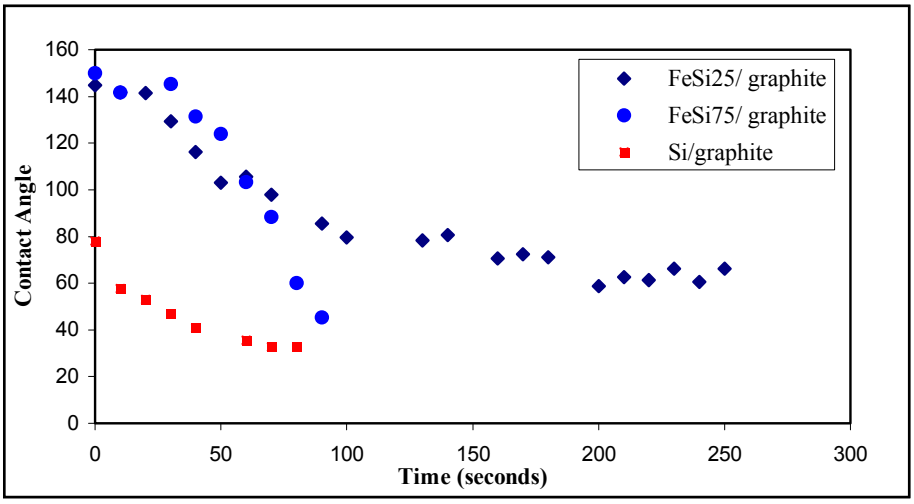

Fig 4 Change in contact angle for different ferroalloys on graphite substrate.

(a) (b)

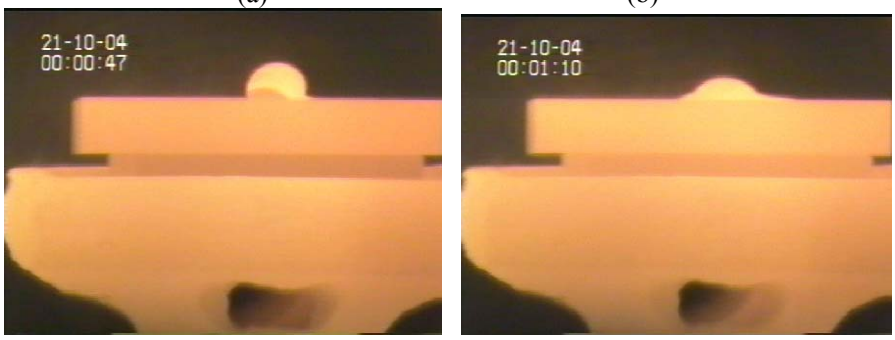

(c)

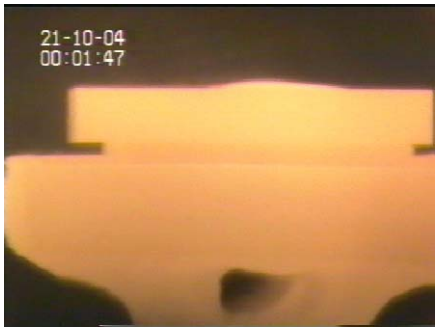

Fig 5. Still image of liquid silicon droplet on graphite substrate (a) droplet 1 s after melting (b) after 23 s c) after 60 s.

(a) (b)

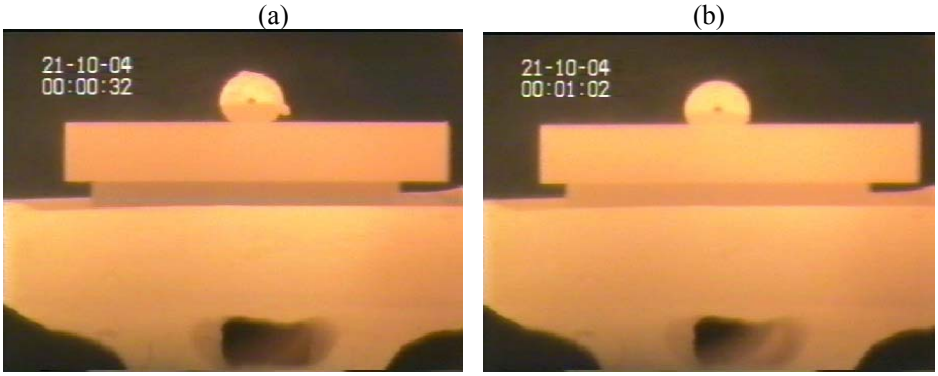

(c)

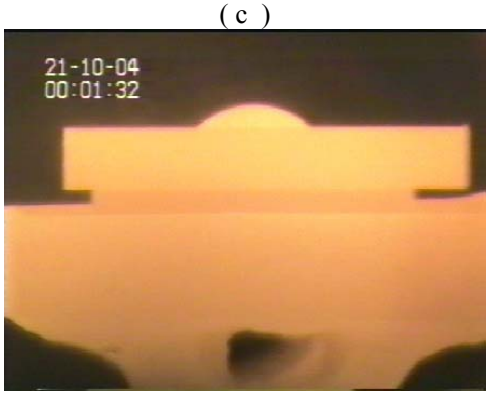

Fig 6. Still image of liquid FeSi75 droplet on graphite substrate (a) droplet 1 s after melting (b) after 30 s c) after 60 s.

(a) (b)

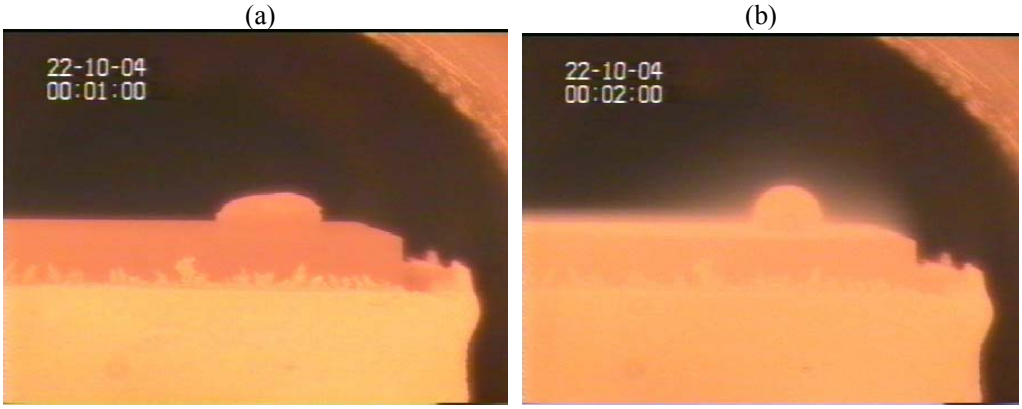

(c)

Fig 7. Still image of liquid FeSi25 droplet on graphite substrate (a) droplet 1 s after melting (b) after 30 s c) after 19 min.

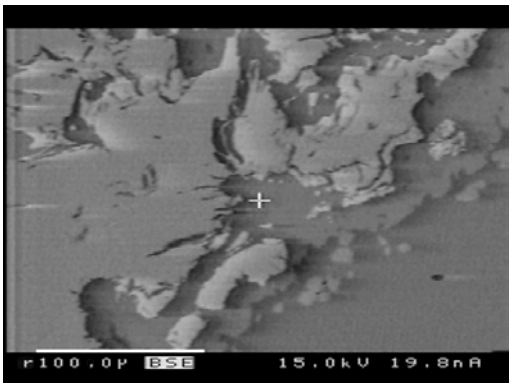

Fig 8. Back-scattered electron image for interface Si-graphite. Cursor is placed on SiC formed at interface.

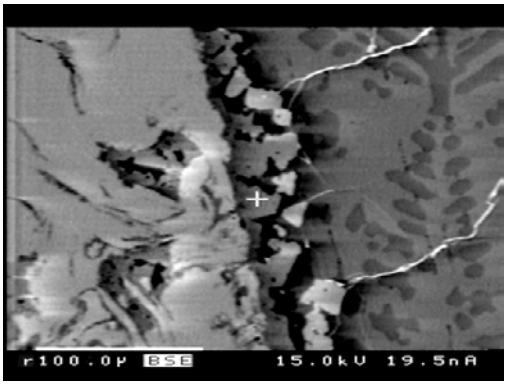

Fig 9. Back-scattered electron image for interface FeSi75-graphite. Cursor is placed on SiC formed at interface.

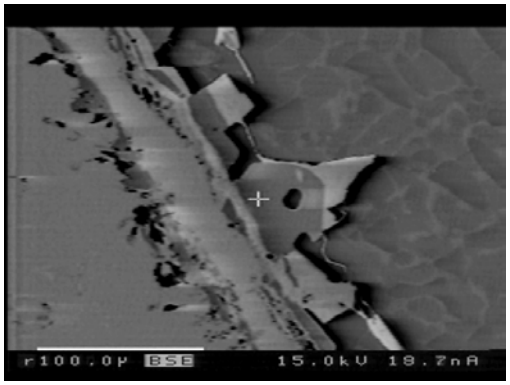

Fig 10. Back-scattered electron image for interface FeSi25-graphite. Cursor is placed on **SiC formed at interface**.